JOURNAL OF MATERIALS SCIENCE 28 (1993) 9–14

Solubility characteristics of synthetic silicate sulphate apatites

K. S. LESHKIVICH, E. A. MONROE
New York State College of Ceramics, Alfred University, Alfred, NY 14802 USA

Isomorphic substitution of (Si, S) for phosphorus in apatite ($Ca_5(PO)_3F$) was investigated in the solid solution series from P-apatite to (Si, S)-apatite utilizing compositions of $Ca_5(PO_4)_{3-x}(SiO_4)_{x/2}(SO_4)_{x/2}F$ with $x = 0, 0.75, 1.5, 2, 2.25, 3$. Study of the solubility characteristics of these apatites showed an increased weight loss in water with progression from the P-apatite end member to the (Si, S)-apatite end member. Experimentally determined pK_{sp} decreased from 60.62 for the fluorapatite ($Ca_5(PO_4)_3F$) to 31.65 for fluorellestadite ($Ca_5(SiO_4)_{1.5}(SO_4)_{1.5}F$). The free energy of formation calculated from the solubility product became less negative from $-6755\ kJ\ mol^{-1}$ for fluorapatite to $-5760\ kJ\ mol^{-1}$ for fluorellestadite.

1. Introduction

Apatite is a generic or family term for materials with the general formula $A_5(XO_4)_3Z$ which crystallizes in the hexagonal system. For this formula, A is a divalent cation, X is a pentavalent cation, and Z is a monovalent anion. Extensive isomorphic substitution can occur at all of the atomic sites, while still preserving the apatite structure. Isomorphic substitutions involving the X sites are of interest for the present study, involving the substitution of the (PO_4^{3-}) group by (SiO_4^{4-}) and (SO_4^{2-}).

Limited investigation of the Si,S-apatites has been reported, primarily concerning the natural minerals. Analysis of the natural minerals of this classification has been reported by McConnel [1], Bredig [2], Vasileva [3], Harada *et al.* [4], and Rouse and Dunn [5]. Limited synthesis of the Si,S-apatites has been reported by Klement and Dihn [6, 7], and Kreidler [8]. Synthesis and crystal chemistry study of the entire solid solution from the P-apatite end member fluorapatite to the (Si,S)-apatite end member fluorellestadite has not been reported. The present study focuses on the synthesis of this solid solution series from $Ca_5(PO_4)_3F$ to $Ca_5(SiO_4)_{1.5}(SO_4)_{1.5}F$ and determination of the solubility characteristics of this solid solution series.

1.1. Solubility data of apatites

The solubility behaviour of synthetic hydroxyapatite and fluorapatite has been investigated by McDowell *et al.* [9], Bell *et al.* [10], and Hagen [11]. The solubility data reported for the P-apatites are summarized in Table I. There has been no investigation reported of the solubility characteristics of the (Si,S)-apatite.

1.2. Free energy of formation of apatites

The free energy of formation of P-apatite has also been determined experimentally and theoretically by several authors. Hagen [11] determined that the free energy of formation of fluorapatite and hydroxyapatite from solubility data were $-6464\ kJ\ mol^{-1}$ for $Ca_5(PO_4)_3F$ and $-6338\ kJ\ mol^{-1}$ for $Ca_5(PO_4)_3OH$, (-1546 and $-1516\ kcal\ mol^{-1}$, respectively). Similarly, Duff [18] had determined the free energy of formation of fluorapatite and hydroxyapatite from brushite-to-apatite transformation studies to be -6372 and $-6247\ kJ\ mol^{-1}$ (-1524.1 and $-1494.2\ kcal\ mol^{-1}$), respectively.

Mikhailov [17] calculated the free energy of formation of various P-apatites on a theoretical basis using standard thermodynamical data. His calculations yielded a free energy of formation for fluorapatite of $-6424\ kJ\ mol^{-1}$ for $Ca_5(PO_4)_3F$ ($-1544\ kcal\ mol^{-1}$). From this calculated value for ΔG_f°, the solubility product for fluorapatite was determined to be $10^{-59.9}$.

2. Experimental Procedure

2.1. Solid state synthesis

The solid solution series from $Ca_5(PO_4)_3F$ to $Ca_5(SiO_4)_{1.5}(SO_4)_{1.5}F$ was synthesized by solid state methods. Six compositions were studied: $Ca_5(PO_4)_{3-x}(SiO_4)_{x/2}(SO_4)_{x/2}F$ with $x = 0, 0.75, 1.5, 2, 2.25, 3$.

The solid state synthesis was based on the reaction

$$uCaO + CaF_2 + xSiO_2 + ySCaSO_4 + zCa_3(PO_4)_2 \rightarrow Ca_5(Si,S,PO_4)_3F \quad (1)$$

where $x + y + 2z = 3$ in the correct stoichiometry for the selected composition, and $u + y + 3z + 1 = 5$. The reactants were $(NH_4)_2SO_4$ and $Ca(OH)_2$, $CaHPO_4$, CaF_2 and dehydrated silica gel.

The reactants, except for CaF_2, were mixed together in the theoretical stoichiometric proportions

0022–2461

TABLE I Summary of solubility Product Data

Investigator	Material[a]	Reference	K_{sp}
Gregory *et al.*	HAP	[12]	3.73×10^{-58}
Clark	HAP	[13]	2.71×10^{-58}
Wier *et al.*	HAP	[14]	2.92×10^{-59}
Driessens	HAP	[15]	1.0×10^{-58}
Verbeek *et al.*	HAP	[16]	3.2×10^{-58}
Hagen	FAP	[11]	1.2×10^{-59}
Mikhailov	HAP	[17]	1.45×10^{-60}
	FAP	[17]	1.58×10^{-60}
Bell *et al.*	HAP	[10]	2.91×10^{-58}
McDowell	HAP	[9]	3.04×10^{-59}
Duff	FAP	[18]	1.20×10^{-59}
	HAP	[18]	2.19×10^{-58}

[a] FAP = fluorapatite, HAP = hydroxyapatite.

with a mortar and pestle. The mixture was pre-reacted at 700 °C for 2 h, forming the intermediate compounds CaO, $CaSO_4$, SiO_2 and $Ca_3(PO_4)_2$. Two subsequent firings and regrindings were performed at 800 and 900 °C for 15 h each. CaF_2 was then added to the intermediate material and the reactants were reground and pressed into a pellet. The pellets were fired in a closed alumina crucible at 1000 °C for 2 h.

2.2. X-ray diffraction phase identification

Powder X-ray diffraction (XRD) data were collected on a Phillips X-ray diffractometer (Phillips Norelco) using CuK_α radiation from 10–60° 2θ at a scanning rate of 0.02° 2θ with a count time of 1 s. Phase purity was determined for a material by comparing its diffraction pattern with JCPDS patterns.

2.3. Phase stoichiometry

The stoichiometry of the products was determined by gravimetric chemical analysis and a fluoride-ion selective electrode. Calcium was determined by the ammonium oxalate–oxalic acid method of Hillebrand and Lundell [19], with calcium being determined as calcium oxalate monohydrate precipitated at a pH of 5.0. Phosphorus was determined as magnesium phosphate ignited to pyrophosphate ($Mg_2P_2O_7$) by the method of Hillebrand [19]. Sulphur was determined with the Leco apparatus. Silicon was determined by the method of boric acid/perchloric acid mixture, and weighed as precipitated silica according to the method of Hillebrand.

For determination of fluoride-ion content, the Orion fluoride-ion activity electrode was used with the pH/ORP Controller (Cole-Parmer). Standards were prepared from 0.1 M l^{-1} stock fluoride solution. 0.1 g sample was dissolved in HNO_3 and diluted with distilled water to 500 ml. Sample pH was adjusted to 6.0–6.5 with HNO_3 and NaOH. To all standards and samples, 50% by volume of total ionic strength adjustment buffer (TISAB) was added to provide a constant background ionic strength, decomplex fluorine, and adjust the solution pH. The sample and standard potential was measured using the fluoride-ion selective electrode. Stable millivolt readings were obtained within 1 min of solution contact with the electrode. The calibration curve technique was used to determine the concentrations. The electrode was recalibrated every hour to maintain the slope of 54–60 mV per decade.

2.4. Dissolution studies: weight loss determination

In order to determine the time period required for attainment of equilibrium, the weight loss of the solid in a buffered solution was determined. A powder sample of 0.04 g, sieved to less than 325 mesh, was placed in 40 ml Tris hydroxy-methylaminomethane (THAM) buffer solution in glass weighing bottles with ground glass seals at 37 °C. The THAM was prepared by adding 500 ml 0.1 M THAM to 466 ml 1 M HCl, and diluting to 1 l. The initial pH of the buffer solution was 6.0 so that the final equilibrium pH would be in the 6–8 pH range.

Each data point for the plot of weight loss versus time was determined by a completely independent experiment. After the time period specified, the suspensions were filtered through sintered glass crucibles with several washes with deionized water followed by a wash with isopropyl alcohol. The sintered glass crucibles were then dried at 100 °C for 16 h. The weight loss versus time was determined using gravimetric methods.

2.5. Hydrolysis of the solid solution compositions

Powder samples of 0.1 g for each composition, sieved to < 325 mesh, were placed in 100 ml deionized water at 27 °C in a glass beaker. The solutions were constantly stirred with a magnetic stirrer throughout the experiment. The initial pH was measured and subsequent measurements were taken at 15 s time intervals up to 150 s. Additional pH measurements were taken at 180, 210, 240, 300, 360, 420, 480, 540, 600 s and 2, 4, 6, 16 and 68 h.

2.6. Solubility product determination

Each data point for the solubility studies was determined by an independent experiment. Powdered samples, sieved to less than 325 mesh, were equilibrated in THAM buffer solution in glass weighing bottle with ground glass seals at 37 °C for 10 and 15 days. The pH of the THAM buffer was initially 6.0 so that the final equilibrated pH would be in the biological pH range of 6–8. After the predetermined time period for equilibration, the suspensions were filtered through sintered glass crucibles and the pH of the filtrate was measured. The weight loss versus time for each sample was determined by gravimetric methods. The concentrations of phosphorus sulphur, silicon, calcium and fluorine were measured in the filtrates. Calcium and silicon were determined by atomic absorption spectroscopy. Phosphorus was determined by the phosphovanado-molybdate method described

by Vogel [20] with a spectrophotometer. Sulphur was determined using nephelometric methods (turbidimetry). Fluorine was determined using an ion-specific electrode.

The following solubility equilibria are established when Ca–P–Si–S species are dispersed in an aqueous medium:

$$Ca^{2+} + OH^- = CaOH^+ \quad K_1 = 10^{1.40} \quad (2)$$

$$CaOH^+ + OH^- = Ca(OH)_2 \quad K_2 = 10^{1.37} \quad (3)$$

$$Ca^{2+} + HPO_4^{2-} = CaHPO_4 \quad K_3 = 382\ [12] \quad (4)$$

$$Ca^{2+} + H_2PO_4^- = CaH_2PO_4^+ \quad K_4 = 4.5\ [12] \quad (5)$$

$$Ca^{2+} + PO_4^{3-} = CaPO_4^- \quad K_5 = 2.9 \times 10^6 \quad (6)$$

$$HPO_4^{2-} = PO_4^{3-} + H^+ \quad K_6 = 6.92 \times 10^{-13}\ [21] \quad (7)$$

$$H_2PO_4^- = HPO_4^{2-} + H^+ \quad K_7 = 6.59 \times 10^{-8}\ [21] \quad (8)$$

$$H_3PO_4 = H_2PO_4^- + H^+ \quad K_8 = 6.18 \times 10^{-3}\ [21] \quad (9)$$

$$H_4SiO_4 = H^+ + H_3SiO_4^- \quad K_9 = 1.995 \times 10^{-10} \quad (10)$$

$$H_3SiO_4^- = H^+ + H_2SiO_4^{2-} \quad K_{10} = 1.995 \times 10^{-12} \quad (11)$$

$$H_2SiO_4^{2-} = H^+ + HSiO_4^{3-} \quad K_{11} = 1 \times 10^{-12} \quad (12)$$

$$HSiO_4^{3-} = H^+ + SiO_4^{4-} \quad K_{12} = 1 \times 10^{-12} \quad (13)$$

$$H_2O = H^+ + OH^- \quad K_{13} = 2.485 \times 10^{-14}\ [21] \quad (14)$$

Because the total calcium concentration is equal to the sum of the concentrations of all calcium species, it follows that

$$[Ca] = (Ca^{2+}) + (CaOH^+) + (Ca(OH)_2) + (CaHPO_4) + (CaH_2PO_4^+) + (CaPO_4^-) \quad (15)$$

Similarly, we can see that

$$[P] = (PO_4^{3-}) + (HPO_4^{2-}) + (H_2PO_4^-) + (H_3PO_4) + (CaH_2PO_4^+) + (CaPO_4^-) \quad (16)$$

Therefore, we can rewrite the above equations as the following:

$$[Ca] = (Ca^{2+})\left[\frac{1}{\gamma Ca^{2+}} + \frac{K_1K_{13}}{(H^+)\gamma CaOH^+} + \frac{K_1K_2K_{13}^2}{(H^+)^2}\right] + (PO_4^{3-})\left[\frac{K_3(H^+)}{K_6} + \frac{K_4(H^+)^2}{K_6K_7\gamma CaH_2PO_4^+} + \frac{K_5}{\gamma CaPO_4^-}\right] \quad (17)$$

and

$$[P] = (PO_4^3)\left[\frac{1}{\gamma PO_4^3} + \frac{(H^+)}{K_6\gamma HPO_4^2} + \frac{(H^+)^2}{K_6K_7\gamma H_2PO_4} + \frac{(H^+)^3}{K_6K_7K_8}\right] + (Ca^{2+})\left[\frac{K_3(H^+)}{K_6} + \frac{K_4(H^+)^2}{K_6K_7\gamma CaH_2PO_4^+} + \frac{K_5}{\gamma CaPO_4^-}\right] \quad (18)$$

where square brackets denote the concentration, γ is the molar activity coefficient, and parentheses indicate the molar activity. Other species of silicon were neglected considering the small values of the solubility products for the pertinent equations and the negligible amounts for any species present. The presence of hydroxyl ions, ionic phosphate species, and calcium phosphate ion pairs was taken into account. The ionic strength was determined by

$$I = \tfrac{1}{2}\sum_i m_i z_i^2 \quad (19)$$

where I is the ionic strength of the solution, m the molar concentration and z the valence. The activity coefficient, γ_i of a z_i valent ion, x_i, was calculated from the Debye–Hückel equation

$$-\log\gamma_i = \frac{AZ_i^2I^{1/2}}{1 + Ba_iI^{1/2}} \quad (20)$$

where A and B are temperature-dependent constants equal to 0.5242 and 0.3318×10^8 at 37 °C, I is the ionic strength, and a_i represents the distance of closest approach for the ith ion. The values used for a_i ($\times 10^8$) from Kaufman [21] are: 9 (H^+), 6.3 (Ca^{2+}), 4.5 ($H_2PO_4^-$), 3.5 (F^-), 4.0 (HPO_4^{2-}, PO_4^{3-}, OH^-), and from Greenberg [22], 4.0 ($H_2SiO_4 = H_3SiO_4^-$).

Values for (Ca^{2+}) and (PO_4^{3-}) were obtained by solving Equations 17 and 18 for [Ca] and [P]. The solubility product for the selected compositions was determined using the expression

$$K_{sp} = (Ca^{2+})^5(XO_4^{3-})^3(F^-) \quad (21)$$

where X = P, Si, S in the appropriate percentages.

2.7. Free energy of formation

The free energy of formation for the selected compositions was determined according to the equations

$$-RT\log K = \Delta G_r \quad (22)$$

$$\Delta G_r = \Delta G_f\ (\text{products}) - \Delta G_f\ (\text{reactants}) \quad (23)$$

where $R = 8.314$, T is the temperature, K the solubility product, and ΔG_r the free energy of reaction.

3. Results and discussion

3.1. Phase identification and stoichiometry

Phase-pure samples were obtained for all selected compositions in the fluorapatite–fluorellestadite solid solution series. The compositions synthesized were very close to theoretical stoichiometry as shown in Table II.

TABLE II Stoichiometry (mole per unit cell)

Ion	Composition (mol % Pvs(Si,S))					
	$P_0(Si,S)_{100}$	$P_{25}(Si,S)_{75}$	$P_{33}(Si,S)_{67}$	$P_{50}(Si,S)_{50}$	$P_{75}(Si,S)_{25}$	$P_{100}(Si,S)_0$
Si	3.195	2.44	1.97	1.52	0.78	0.0
S	2.997	2.32	2.18	1.67	0.85	0.0
P	0.0	1.20	2.05	2.97	4.46	6.02
Ca	9.828	9.82	9.81	9.88	9.79	10.14
Ca:(P,Si,S)	1.59	1.65	1.58	1.60	1.60	1.68

3.2. Dissolution studies: weight loss

The weight loss versus time in buffered water for all six compositions showed an initially high rate of dissolution with a general trend of increasing weight loss rate versus increasing percentage substitution of (Si,S) for phosphorus through the solid solution series. Fig. 1 illustrates this trend. The initial high rate of dissolution can be accounted for by two factors: (1) the initial pH of the buffered solutions was acidic in order to maintain the final solution pH after equilibration within a narrow pH range, therefore the initial solubility is greater because of the initially more acidic solutions; (2) the smaller particles present would exhibit a higher solubility than the larger particles, described by the Gibbs–Kelvin equation and these same particles could be consumed early on. The decrease and levelling off of the solubility can be accounted for by the accumulation of reaction products and the rise in pH to a state of equilibrium and to the elimination of the very fine particles.

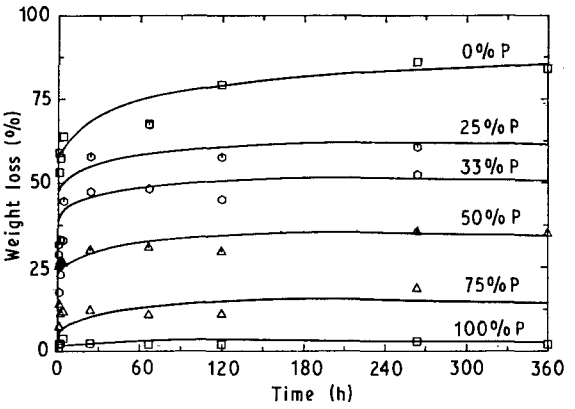

Figure 1 Weight loss versus time in aqueous solution for solid solution series.

3.3. Hydrolysis and pH change

Fig. 2 shows the behaviour of the solid solution series in water. The hydrolysis reactions resulting in the rise in pH are rapid. Within 1 h, the solution pH had stabilized. With increasing substitution of (Si,S) for phosphorus, there is an increase in the final pH value to which the sample hydrolyses. This is likely due to the ions (PO_4^{3-}), (SiO_4^{4-}) and (SO_4^{2-}) which hydrolyse basic. The 50% and 0% phosphorus solid solutions contain more species of these basic ions because their solubility is greater, and therefore there is a higher resultant pH. X-ray diffraction data of the precipitate that formed from these compositions in water indicated formation of a calcium silicate as well as calcium carbonate.

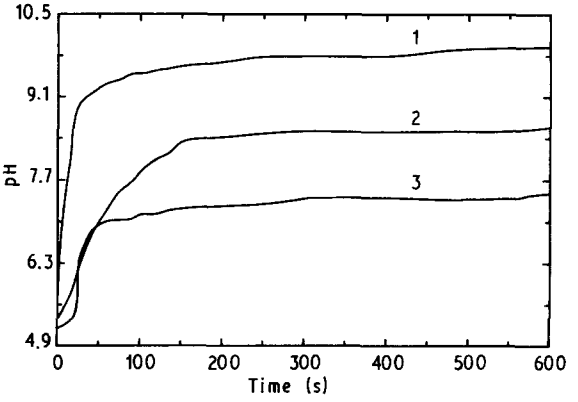

Figure 2 pH versus time in aqueous solution for the solid solution series: 1 = 0%P, 2 = 50%P, 3 = 100%P.

3.4. Solubility product

The chemical analysis results of the concentration of the ionic species are listed in Table III. The stoichiometry of the powder present in the saturated solution may be demonstrated by a "potential diagram". The coordinates are defined as $-\log[(Ca^{2+})(OH^-)^2]$ and $-\log[(H^+)^3((Si,S,P)O_4^{3-})]$. The saturation condition is defined as a straight line, whose slope is the negative of the Ca/(Si,S,P) ratio in the solid. The 0% and 100% phosphorus solids did show congruent dissolution, as well as saturation with respect to the solid. The slopes of the 0%, 50% and 100% phosphorus compositions were 1.75, 1.12 and 1.50. This observation indicates that the 50% phosphorus solid did not show congruent dissolution in comparison with the 0% and 100% phosphorus solids (Fig. 3). These results are similar to those of Bell *et al.* [10] in solubility studies of hydroxyapatite. They determined that hydroxyapatite had a constant solubility product even though non-stoichiometric dissolution of the solid was evident. Similarly, Kaufman and Kleinberg [21], determined that there was non-stoichiometric dissolution of hydroxyapatite, but the solubility product remained in a constant range.

The calculated pK_{sp} values for the selected compositions calculated from the experimentally obtained ionic concentration data resulted in average values as

TABLE III Solubility (concentration (M L^{-1}) and weight loss)

%P	Sample	Days	F ($\times 10^{-4}$)	Si ($\times 10^{-3}$)	S ($\times 10^{-3}$)	Ca ($\times 10^{-2}$)	P ($\times 10^{-4}$)	pH	Wt loss (%)
100	5	10	0.13			0.072	0.564	5.52	2.0
	6	15	0.06			0.072	0.141	5.57	0.25
	7	15	0.30			0.072	0.282	5.27	2.0
50	2	15	2.99	2.84	1.185	1.073	2.874	6.48	35.5
	3	21	1.75	5.34	2.682	1.497	1.614	7.26	29.2
	4	21	3.10	5.69	2.682	1.522	3.228	7.24	29.4
0	14	10	1.45	4.27	1.684	10.130		6.96	80.0
	9	11	3.40	2.67	0.842	8.184		6.76	95.8
	11	11	3.60	2.84	0.374	8.034		6.43	90.9
	13	15	4.20	4.27	1.497	8.683		7.03	89.5
	8	21	2.10	4.98	4.990	6.088		6.71	78.3
	12	21	3.60	2.13	0.312	7.909		7.86	75.2
	10	15	2.10	4.27	2.994	8.683		5.71	84.0

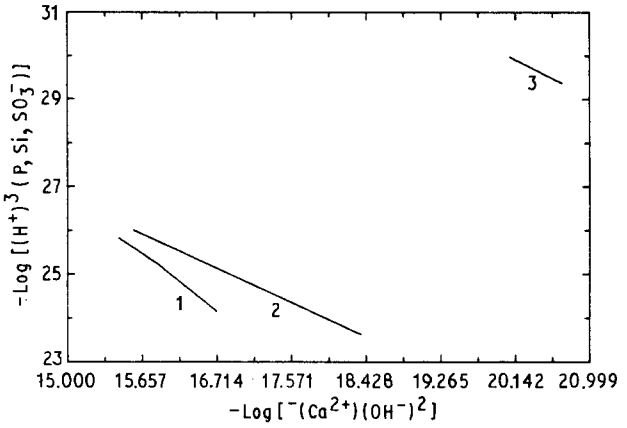

Figure 3 Congruent dissolution potential diagram for solid solution series: 1 = 0%P, 2 = 50%P, 3 = 100%P.

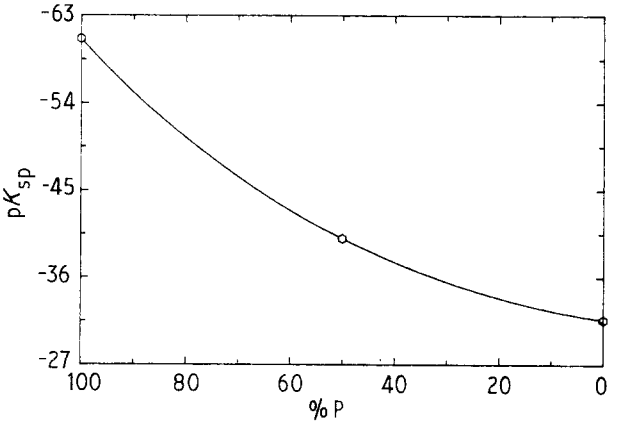

Figure 4 Solubility versus composition of solid solution series.

follows

$Ca_5(PO_4)_3F$	60.62
$Ca_5(PO_4)_{1.5}(SiO_4)_{0.75}(SO_4)_{0.75}F$	40.02
$Ca_5(SiO_4)_{1.5}(SO_4)_{1.5}F$	31.65

There is as trend of increasing solubility (decreased pK_{sp}) with increased per cent substitution of (Si,S) for phosphorus (see Fig. 4). This trend can be attributed to the associated change in lattice energy with this substitution type, which increases with increasing ionic charge and decreases with increasing ionic size. With substitution of Si^{4+} and S^{6+} for P^{5+}, there is a decrease in the overall lattice energy. The effect of this reduced lattice energy was seen in the melting points determined for the solid solution series. From the 100% phosphorus composition to the 0% phosphorus composition, there was a corresponding decrease in the melting point as the percentage of silicon and sulphur which was substituted for the phosphorus increased. This indicated a reduced lattice bonding with increased substitution of (Si,S) for phosphorus. The hydration energy of the substituted ions affects the solubility in that the hydration energy is largest for small highly charged ions. S^{6+}, having a radius of 0.029 nm, would have a very high hydration energy compared to P^{5+}, which has a radius of 0.035 nm. Si^{4+}, with a radius of 0.04 nm, would have the lowest hydration energy. The combined effect of the lattice energy and the hydration energy of the substituted ions resulted in increased solubility from 100% phosphorus to 0% phosphorus composition of the solid solution series.

The K_{sp} of the composition in the centre of the solid solution range is not intermediate in value, as expected. When two salts MA and MB are mixed, resulting in a true homogeneous solid solution, the equilibrium between the solid and an aqueous solution of its ions can be described at equilibrium. When a solid solution is placed in water, the following relationships apply according to Berndt and Stearns [22]

$$\frac{[A^-]_{eq}}{[B^-]_{eq}} = \frac{xK_{MA}}{1 - xK_{MB}} \tag{24}$$

and

$$[M^{2-}]_{eq}[A^-]^x_{eq}[B^-]^{(1-x)}_{eq} = K^x_{MA}K^{(1-x)}_{MB}x^x(1x)^{1-x} \tag{25}$$

where K_{MA} and K_{MB} are the solubility products of pure MA and MB. The solubility will always be less than the solubility of the physical mixture of MA and MB which would be calculated to be $(K_{MA} + K_{MB})^{1/2}$.

This is to be expected because the solid solution has extra stability due to the entropy of mixing. If $K_{MA} > K_{MB}$, the liquid solution will always be richer in the more soluble ion A^-. For the centre member of the investigated apatite solid solution, a physical mixture would result in a calculated pK_{sp} value of 15.82, whereas the calculated K_{sp}, according to the solid solution equations above, results in a value of $pK_{sp} = 46.44$ which is lower solubility (K_{sp}). This result is in close agreement with the experimentally obtained value of $pK_{sp} = 40.02$.

3.5. Free energy of formation

The free energy of formation calculated from the solubility product for the selected compositions was determined to be:

$Ca_5(PO_4)_3F$ $-6755\ kJ\ mol^{-1}(-1615\ kcal\ mol^{-1})$

$Ca_5(PO_4)_{1.5}(SiO_4)_{0.75}(SO_4)_{0.75}F$

$-6235\ kJ\ mol^{-1}(-1490\ kcal\ mol^{-1})$

$Ca_5(SiO_4)_{1.5}(SO_4)_{1.5}F$

$-5760\ kJ\ mol^{-1}(-1377\ kcal\ mol^{-1})$

The calculated value for the 100% phosphorus end-member correlates well with literature values for fluorapatite of -1544 [17] and $-1546\ kcal\ mol^{-1}$ [11]. As expected from the solubility data, where solubility increases with increasing substitution of (Si,S) for phosphorus, there is a less negative ΔG_f with increasing substitution of (Si,S) for phosphorus.

5. Conclusion

Powder samples of the solid solution compositions placed in water showed rapid hydrolysis of the (Si,S)-containing compositions resulting in a rapid pH rise. The compositions with (Si,S) > P had a higher resultant pH than the compositions with P > (Si,S). The increase in pH can be attributed to the SiO_4 ions which are basic ions that bind H^+ to give more free (OH^-) ions in water.

With progression from the P-apatite end member towards the (Si,S)-apatite end member, there was an increasing weight loss with time in aqueous solution, indicative of the increased solubility. The pK_{sp} of the solid solution series decreased from 60.62 for fluorapatite to 31.65 for fluorellestadite. The free energy of formation became less negative from $-6755\ kJ\ mol^{-1}$ for the P-apatite end member to $-5760\ kJ\ mol^{-1}$ for the (Si,S)-apatite end member.

References

1. D. McCONNELL, *Amer. Mineral.* **22** (1937) 977.
2. M. BREDIG, *Z. Anorg. Allgem. Chem.* **230** (1936) 750.
3. Z. VASILEVA, *Geochem.* **118** (1958) 464.
4. K. HARADA, K. NAGASHIMA and A. KATO, *Amer. Mineral.* **56** (1971) 1507.
5. R. ROUSE and P. DUNN, *ibid.* **67** (1982) 90.
6. R. KLEMENT, *Naturwiss.* **27** (1939) 57.
7. R. KLEMENT and P. DIHN, *Ber. Bunsenges Phys. Chem.* **48** (1942) 334.
8. E. KREIDLER, PhD thesis, Marquette University, Milwaukee, WI (1974).
9. H. McDOWELL, T. GREGORY and W. BROWN, *J. Res. Nat. Bur. Stand.* **81A** (1977) 273.
10. L. BELL, H. MIKA and B. KRUGER, *Arch. Oral Biol.* **23** (1978) 329.
11. A. HAGEN, *J. Dent. Res.* **54** (1975) 384.
12. T. GREGORY, E. MORENO and W. BROWN, *J. Res. Nat. Bur. Stand.* **74A** (1970) 461.
13. J. S. CLARK, *Can. J. Chem.* **33** (1955) 1969.
14. D. R. WIER, CHIEN, S. H. and BLACK, C. A., *Soil Sci.*, **111** (1971) 107.
15. F. DRIESSENS, *Ber. Bunsenges Phys. Chem.* **82** (1978) 312.
16. R. VERBEEK, H. STEGAER, H. P. THUN and F. VERBEEK, *J. Chem. Soc. Lond.* **76** (1980) 209.
17. A. MIKHAILOV, *Russ. J. Phys. Chem.* **41** (1967) 461.
18. E. DUFF, *J. Inorg. Nucl. Chem.* **34** (1972) 101.
19. W. F. HILLEBRAND, in "Applied Inorganic Analysis" (John Wiley, New York, 1953) pp. 671–883.
20. A. I. VOGEL, "Quantitative Inorganic Analysis" (Longmans Green, London, 1962) p. 810.
21. H. KAUFMAN and I. KLEINBERG, *Calcif. Tissue. Int.* **27** (1979) 143.
22. A. BERNDT and R. STEARNS, *J. Chem. Ed.* **50** (1973) 415.
23. G. EWING, "Instrumental Methods of Chemical Analysis", 2nd Edn (McGraw Hill, New York, 1960) pp. 15–74.
24. G. LEVINSKAS and N. NEUMAN, *J. Phys. Chem.* **59** (1955) 164.
25. S. GREENBERG and T. CHANG, *J. Phys. Chem.* **69** (1965) 182.

Received 9 January 1991
and accepted 1 May 1992